Biochimica et Biophysica Acta 1822 (2012) 248–260

Contents lists available at SciVerse ScienceDirect

Biochimica et Biophysica Acta

journal homepage: www.elsevier.com/locate/bbadis

MiR-21 is involved in cervical squamous cell tumorigenesis and regulates CCL20

Tingting Yao, Zhongqiu Lin *

Department of Gynecological Oncology, Sun Yat-sen Memorial Hospital, Sun Yat-sen University, 107 Yan Jiang West Road, Guangzhou 510120, People's Republic of China
Key laboratory of malignant tumor gene regulation and target therapy of Guangdong Higher Education Institutes, Sun Yat-sen University, People's Republic of China

ARTICLE INFO

Article history:
Received 1 April 2011
Received in revised form 29 September 2011
Accepted 30 September 2011
Available online 7 October 2011

Keywords:
Cervical squamous carcinoma
Cervical intra-epithelial neoplasia
Human papillomavirus
MIR21
CCL20

ABSTRACT

MicroRNA 21 (miR-21) has been implicated in various aspects of carcinogenesis. However, its function and molecular mechanism in cervical squamous carcinoma have not been studied. Using TaqMan quantitative real-time PCR and Northern blot, we confirmed that miR-21 is significantly overexpressed in human cervical squamous cancer tissues and cell lines. Remarkably, we showed that the level of miR-21 correlates with the tumor differentiation and nodal status by ISH. Furthermore, we demonstrated that miR-21 regulates proliferation, apoptosis, and migration of HPV16-positive cervical squamous cells. In order to identify candidate target genes for miR-21, we used gene expression profiling. By luciferase reporter assays, we confirmed that CCL20 is one of its target genes, which is related to the HPV16 E6 and E7 oncogenes. Our results suggest that miR-21 may be involved in cervical squamous cell tumorigenesis.

1. Introduction

Cervical carcinoma is second only to breast cancer in female malignancies worldwide [1,2]. Hence, it poses an important public health problem. Approximately 80% of primary cervical cancers arise from pre-existing squamous dysplasia. The most important etiologic agent in the pathogenesis is human papillomavirus (HPV). However, not all women infected with high-risk HPV develop cervical carcinoma. This suggests that other cofactors must be present in the pathogenic pathway between cervical dysplasia and carcinoma.

MicroRNAs (miRNAs) are a class of endogenous small, non-coding RNA molecules of about 21 to 23 nucleotides that have the capacity to specifically inhibit translation or induce mRNA degradation, predominantly through targeting the 3′ untranslated regions (UTRs) of mRNA. Abnormal expression levels of miRNAs are associated with a variety of human cancers [3]. One of these microRNAs, miR-21, is a key player in human cancers, including breast [4], prostate [5], pancreatic [6] and colon cancer [7]. This miRNA has been linked to tumor aggression and carcinogenesis as an oncogene. Inhibition of miR-21 in tongue squamous cell increases expression of Tropomyosin1 (TPM1), suppresses tumor growth and induces apoptosis [8]. Knockdown of miR-21 upregulates programmed cell death 4 (PDCD4), causing significant reduction in invasion and metastasis [9–11]. It has been reported that miR-21 is overexpressed and promotes cell proliferation and down-regulates the expression of programmed cell death 4 (PDCD4) in HeLa cervical carcinoma cells [12,13]. However, the expression of miR-21 and its target gene has not been reported in squamous cervical carcinoma. Whether miR-21 has relationship with HPV remains elusive. Furthermore, miRNAs share only partial complementarity to their targets, and the conditions required for miRNA targeting have not been fully established. Identification and validation of the key targets that function in a specific cell setting or process are still a challenge. In this study, we aimed to examine miR-21 expression in HPV16 positive squamous cervical carcinomas. Next, we correlated miR-21 expression with the clinical status. We transfected anti-miR-21 in squamous cervical carcinoma cell lines, Caski and Siha, and investigated its contribution to tumor cell growth, apoptosis and migration. We also evaluated the role of miR-21 in tumor formation in immunocompromised mice inoculated subcutaneously. Bioinformatic analysis was used to screen and identify various genes with miR-21 target sites. Luciferase activity assays indicated that CCL20 contains putative miR-21 binding sites. Furthermore, introduction of miR-21 could reduce the expression of CCL20 protein and CCL20 mRNA in SCC cell lines.

2. Materials and methods

2.1. Patients and tissue

Paired cervical tumors (intra-epithelial neoplasia or primary cervical squamous carcinomas) and adjacent normal tissues were obtained from 126 patients (Table 1), who were admitted to the Department of Gynecologic Oncology of Sun Yat-sen Memorial Hospital, Sun Yat-sen University, from January 2002 to June 2011. None of the patients recruited into the present study received radiotherapy or chemotherapy

* Corresponding author at: Department of Gynecological Oncology, Sun Yat-sen Memorial Hospital, Sun Yat-sen University, 107 Yan Jiang West Road, Guangzhou 510120, People's Republic of China. Tel.: +86 13802921545; fax: +86 20 81332853.
E-mail address: linzhongqiu@hotmail.com (Z. Lin).

0925-4439/$ – see front matter © 2011 Elsevier B.V. All rights reserved.
doi:10.1016/j.bbadis.2011.09.018

Table 1
Summary of demographic and clinicopathologic features in human cervical tumors.

No.	Age	Cell type	FIGO Stage	HPV	Tumor diameter	Lymph nodal metastasis	Parametrial invasion	Vessel invasion	Differentiation	MiR-21
1	34	SCC	Ib1	16	3 cm	−	−	+	Poor	+
2	50	SCC	Ib1	16	Erosion	−	−	−	Poor	+
3	56	SCC	Ib1	16	1.5 cm	−	−	−	Well	−
4	39	SCC	Ib1	16, 18	2 cm	−	−	+	Mediate	+
5	48	SCC	Ib1	16, 31	Erosion	−	−	−	Poor	+
6	40	SCC	Ib2	16	4 cm	−	−	−	Well	+
7	61	SCC	Ib1	16	3 cm	−	−	+	Poor	+
8	42	SCC	Ib1	16, 33	2.3 cm	−	−	+	Poor	++
9	33	SCC	Ib1	16	Erosion	−	−	+	Poor	++
10	42	SCC	Ib1	16	3 cm	−	−	−	Well	−
11	42	SCC	Ib1	16	Erosion	−	−	+	Poor	++
12	50	SCC	Ib1	16	2.5 cm	−	−	−	Poor	+
13	53	SCC	Ib1	16	1 cm	−	−	+	Poor	+
14	52	SCC	Ib2	16, 35	5 cm	−	−	−	Mediate	−
15	40	SCC	Ib1	16	3.5 cm	−	−	−	Poor	+
16	37	SCC	Ib1	16	1 cm	−	−	−	Mediate	++
17	28	SCC	Ib2	16	5 cm	−	−	+	Poor	+
18	52	SCC	IIa	16	2 cm	+	−	−	Poor	++
19	47	SCC	Ib2	16	7 cm	−	−	+	Poor	+
20	40	SCC	Ib1	16	Erosion	+	−	−	Poor	++
21	38	SCC	Ib1	16	1 cm	−	−	−	Mediate	−
22	53	SCC	Ib1	16	3 cm	−	−	+	Poor	+
23	44	SCC	Ib1	16, 39	Erosion	+	−	+	Poor	+
24	50	SCC	IIa	16, 33	4 cm	−	+	−	Well	+
25	38	SCC	Ib1	16	3 cm	+	−	−	Poor	++
26	58	SCC	Ib1	16	Erosion	+	+	+	Poor	++
27	34	SCC	Ib1	16	Erosion	+	+	−	Poor	+
28	31	SCC	Ib2	16	4.5 cm	−	−	+	Poor	−
29	60	SCC	IIa	16	Erosion	−	−	−	Well	+
30	50	SCC	IIa	16	4.7 cm	+	−	+	Poor	+
31	48	SCC	IIa	16	3 cm	+	+	−	Poor	+
32	58	SCC	IIa	16	Erosion	−	−	−	Poor	+
33	50	SCC	IIa	16	5 cm	+	+	+	Poor	++
34	57	SCC	IIa	16	2 cm	+	−	+	Mediate	+
35	37	SCC	Ib2	16	4 cm	+	−	−	Poor	++
36	30	SCC	Ib1	16	2.5 cm	−	−	−	Well	−
37	41	SCC	Ib1	16	Erosion	−	−	−	Poor	−
38	30	SCC	Ib1	16	3 cm	−	−	−	Poor	++
39	40	SCC	Ib1	16	2 cm	−	−	−	Mediate	++
40	40	SCC	Ib1	16	Erosion	−	−	−	Mediate	+
41	53	SCC	Ib1	16, 18	3 cm	−	−	+	Poor	+
42	50	SCC	Ib1	16, 18	2 cm	−	−	−	Mediate	++
43	50	SCC	Ib1	16	1.5 cm	−	−	−	Well	+
44	47	SCC	Ib1	16	4 cm	−	−	+	Poor	++
45	52	SCC	Ib1	16	Erosion	+	−	−	Poor	+
46	38	SCC	Ib1	16	3 cm	+	−	−	Mediate	+
47	44	SCC	Ib1	16	3 cm	−	−	+	Poor	++
48	55	SCC	Ib1	16	2.5 cm	−	−	−	Poor	+
49	43	SCC	Ib1	16	Erosion	−	−	−	Well	+
50	38	SCC	Ib1	16	Erosion	−	−	+	Poor	+
51	53	SCC	Ib2	16	5 cm	+	−	+	Poor	+
52	49	SCC	Ib2	16	4 cm	+	−	+	Poor	++
53	53	SCC	Ib2	16	4 cm	−	−	−	Poor	++
54	30	SCC	Ib2	16	4 cm	+	−	+	Poor	+
55	44	SCC	Ib2	16, 45	5 cm	−	−	+	Well	+
56	38	SCC	Ib2	16, 66	6 cm	−	−	−	Mediate	++
57	44	SCC	Ib1	16	2 cm	+	−	+	Poor	+
58	38	SCC	Ib2	16	Erosion	+	−	+	Poor	++
59	28	SCC	Ib1	16	2 cm	−	−	−	Well	−
60	38	SCC	Ib1	16	3 cm	−	−	+	Poor	++
61	53	SCC	Ib2	16	5 cm	+	+	+	Poor	++
62	42	SCC	IIa	16	2 cm	−	−	−	Well	+
63	47	SCC	IIa	16	4 cm	−	−	−	Mediate	−
64	49	SCC	IIa	16	5 cm	+	−	−	Mediate	++
65	55	SCC	Ib1	16	Erosion	+	−	−	Mediate	+
66	46	SCC	IIa	16	4 cm	−	−	+	Mediate	+
67	53	SCC	IIa	16	5 cm	−	−	+	Well	−
68	63	SCC	Ib2	16, 31	4.8 cm	+	+	−	Poor	+
69	52	SCC	IIa	16	5 cm	+	−	+	Poor	++
70	43	SCC	IIa	16	1.5 cm	−	+	+	Well	−
71	30	SCC	Ib1	16	2.5 cm	−	−	−	Well	−
72	38	SCC	IIa	16	2.5 cm	−	−	+	Well	−
73	45	SCC	IIa	16	Erosion	+	−	+	Mediate	+
74	37	SCC	IIa	16	5 cm	−	−	−	Well	−

(continued on next page)

Table 1 (*continued*)

No.	Age	Cell type	FIGO Stage	HPV	Tumor diameter	Lymph nodal metastasis	Parametrial invasion	Vessel invasion	Differentiation	MiR-21
75	43	SCC	IIa	16	6 cm	−	−	−	Well	−
76	51	SCC	IIa	16	2 cm	+	−	+	Poor	−
77	44	SCC	IIa	16	4.5 cm	−	−	+	Mediate	+
78	53	SCC	IIa	16	1 cm	+	−	−	Well	+
79	29	SCC	IIa	16	5 cm	−	+	−	Poor	++
80	30	SCC	IIa	16	4 cm	+	+	−	Poor	+
81	50	SCC	IIa	16	2 cm	+	+	+	Poor	+
82	37	SCC	IIa	16	4.5 cm	−	−	+	Well	−
83	24	SCC	Ib1	16	1 cm	−	−	−	Well	−
84	57	SCC	IIa	16, 68	6 cm	−	−	+	Mediate	+
85	27	CIN	I0	16						−
86	47	CIN	I0	16						+
87	43	CIN	I0	16						−
88	44	CIN	I0	16						−
89	34	CIN	I0	16						−
90	40	CIN	I0	16						−
91	43	CIN	I0	16						−
92	38	CIN	I0	16						−
93	48	CIN	I0	16						−
94	46	CIN	I0	16						−
95	39	CIN	I0	16						−
96	41	CIN	I0	16, 6						−
97	39	CIN	I0	16, 11						−
98	39	CIN	I0	16						−
99	48	CIN	I0	16, 66						−
100	60	CIN	I0	16						−
101	42	CIN	I0	16						−
102	49	CIN	I0	16						−
103	50	CIN	I0	16						++
104	36	CIN	I0	16						−
105	42	CIN	I0	16						+
106	54	CIN	I0	16						+
107	35	CIN	I0	16						−
108	34	CIN	I0	16						+
109	46	CIN	I0	16						−
110	38	CIN	I0	16						+
111	37	CIN	I0	16						−
112	57	CIN	I0	16, 31						+
113	35	CIN	I0	16						−
114	65	CIN	I0	16						+
115	39	CIN	I0	16						−
116	50	CIN	I0	16						+
117	36	CIN	I0	16						−
118	38	CIN	I0	16						−
119	33	CIN	I0	16						+
120	30	CIN	I0	16						−
121	42	CIN	I0	16, 42						−
122	34	CIN	I0	16, 45						+
123	36	CIN	I0	16						−
124	36	CIN	I0	16						−
125	30	CIN	I0	16						−
126	29	CIN	I0	16						−

or any other treatment prior to surgery. All of them were tested using the HybriBio Human Papillomavirus GenoArray Test Kit [14] and infection was confirmed upon hospital admission. Adjacent normal tissue samples were taken at least 1 cm distal to tumor margins. We also chose two cases obtained from patients uninfected with HPV, who were undergoing hysterectomy for hysteromyoma, as normal controls. Tissue histology was independently evaluated by two pathologists. All samples were collected with informed consent according to the internal review and ethics boards of the hospital.

2.2. In situ hybridization

In situ hybridization for miR-21 was performed in 84 paired samples of cervical carcinoma tissues (No.1–No.84) and 42 paired samples of CIN tissues (No.85–No.126) versus matched normal cervical tissues. Paraffin-embedded, formalin-fixed tissue was cut into 5 μm sections and placed on polylysine-coated slides. After deparaffinization, rehydration and fixation, the slides were incubated in proteinase K solution at 37 °C for 15 min. They were then immersed in formaldehyde for 10 min. Slides were prehybridized in hybridization buffer (no probe) at 60 °C for 1 h. Digoxigenin (DIG)-labeled mercury-locked nucleic acid probes for miR-21, U6 (positive control), and scrambled RNA (negative control; Exiqon, Woburn, MA) were hybridized to the slides for 20 h at 60 °C. Following stringency washes at 60 °C and blocking for 1 h at room temperature, sections were incubated for 2 h at room temperature with pre-incubated blocking solution with alkaline phosphatase conjugated anti-DIG Fab fragment, and stored at 4 °C until the following day. Slides were then incubated for 10 h with RTU BM purple AP substrate (Roche, Basel, Switzerland) at room temperature, placed in stop solution for 5 min and mounted. The slides were then scored by two pathologists independently and blindly as negative (−), weak or focally positive (+), or strongly positive (++).

2.3. Immunohistochemistry

Paraffin-embedded, formalin-fixed tissue was cut into 5 μm section, placed on polylysine-coated slides, de-paraffinized in xylene, rehydrated

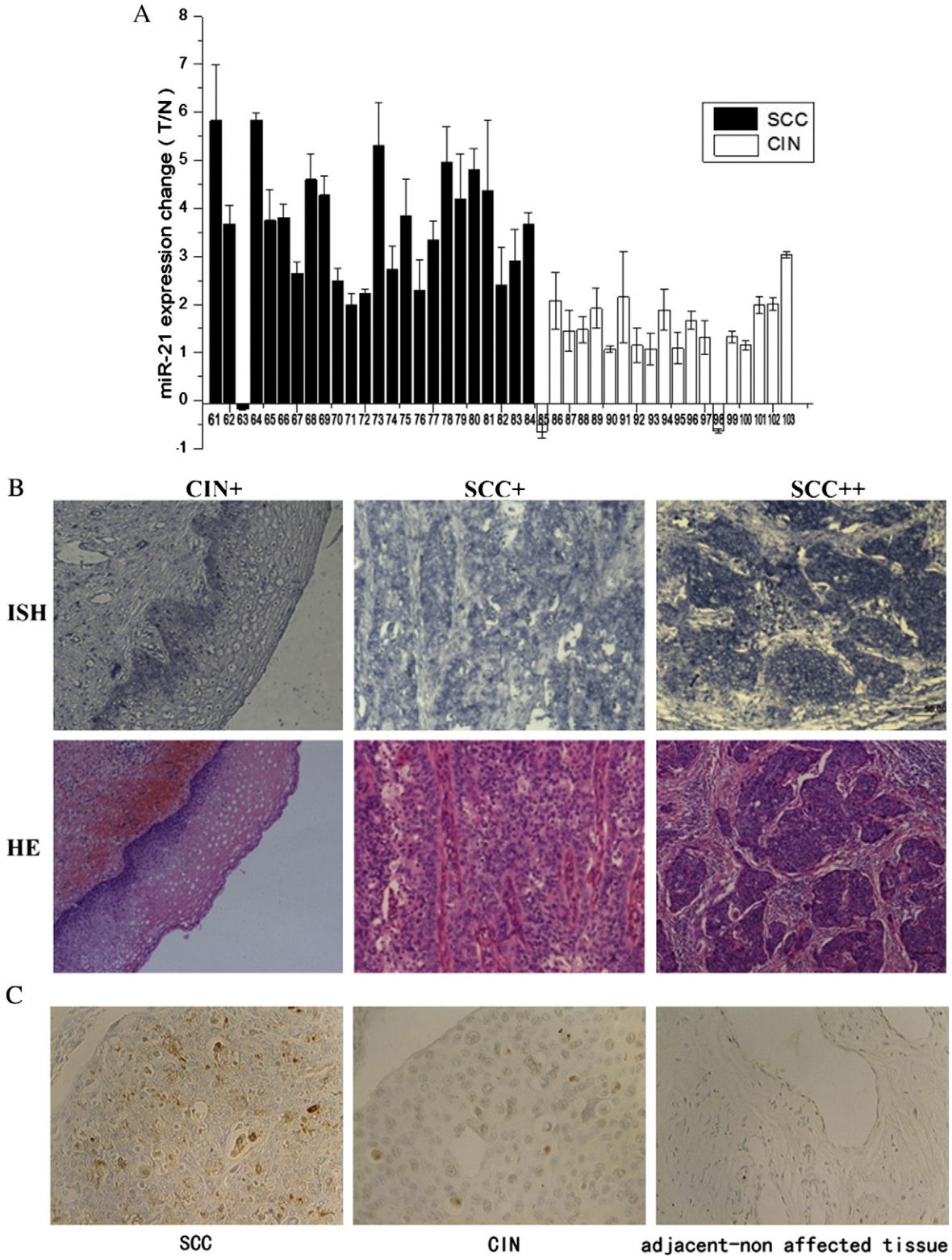

Fig. 1. MiR-21 is upregulated in SCC tissues. (A) Overexpression of miR-21 was verified by qRT-PCR. All patients were divided into two groups as SCC and CIN. Numbers marked at the bottom represent the number of each specimen (columns: miR-21 expression ratio of each tumor specimen to matched adjacent normal tissue; bars, SD from triplicate assays; T: tumor specimen; N: normal tissue). (B) In situ hybridization (top panels; ×100 magnification) and H&E staining (bottom panels; ×100 magnification) of CIN and SCC tissues with + or ++. (C) HPV E6 oncoprotein detected by immunohistochemistry in SCC (left), CIN (middle) and adjacent-non affected (right) tissues (×400 magnification).

through graded ethanol, quenched for endogenous peroxidase activity in 0.3% hydrogen peroxide, and processed for antigen retrieval by microwave heating in 10 mM citrate buffer (pH 6.0). Sections were incubated at 4 °C overnight with anti-HPV16E6 mouse mAb (Abcam). Immunostaining was performed using ChemMate DAKO EnVision Detection Kit, Peroxidase/DAB, Rabbit/Mouse (DakoCytomation, Glostrup, Denmark), which resulted in a brown-colored precipitate at the antigen site. Subsequently, sections were counterstained with hematoxylin

Table 2
The expression of miR-21 in cervical intraepithelial neoplasia and cervical carcinoma by ISH.

Group	Cases (n)	MiR-21			
		−	+	++	Positive (%)
Cervical intraepithelial neoplasia	42	31	10	1	26.19
Cervical carcinoma	84	18	42	24	78.57

(Zymed Laboratories, South San Francisco, CA) and mounted in non-aqueous mounting medium. The primary antibody was omitted for negative controls. The outcome status was classed as positive for HPV-16 if a punctate signal specific to the tumor cell nuclei was present.

2.4. Quantitative real-time PCR

Quantitative real-time reverse transcription PCR (qRT-PCR) for miR-21 was performed in 24 paired samples of cervical squamous carcinoma tissues (No.61–No.84) and 19 paired samples of CIN tissues (No.85–No.103) versus matched normal cervical tissues. For corresponding normal tissue we used adjacent non-affected tissue from the same resected specimens. All reactions were done in a 20 μL reaction volume in triplicate by SYBR Green Real-time PCR Universal Reagent (GenePharma Co., Ltd.) and analyzed by MX-3000P Real-time PCR machine (Stratagen). Standard curves were generated and the relative amount of miR-21 was normalized to U6 snRNA ($2^{-\Delta Ct}$). MiR-21 expression fold-change was evaluated using $2^{-\Delta\Delta Ct}$. Primers for miR-21 and U6 snRNA were as follows: miR-21 (forward, GGACTAGCTTATCAGACTG; reverse, CATCAGATGCGTTGCGTA) and U6-snRNA (forward, ATTGGAACGATACAGAGAAGAT; reverse, GGAACGCTTC ACGAATTT). Probes for miR-21 and U6 snRNA were as follows: FAM-TGGCCCCTGCGCAAGGATG-DABCYL and FAM-CGCACCGCGTCAACATCA GGGTGCG-DABCYL, respectively [8].

Primer sequences for detection were as follows: HPV16E6 (forward, 5′-GAGAACTGCAATGTTTCAGGACC-3′; reverse, 5′-TGTATAGTTGTTTGCAGCTCTGTGC-3′), CCL20 (forward, 5′-GCGAATCAGAAGCAGCAAGC-3′; reverse, 5′-CTTCATTGGCCAGCTGCC-3′), ALDH3A1 (forward, 5′-GAGGCCTCTGATGAATGA-3′; reverse, 5′-TCCGATGGGACACAGTAT-3′), CRYAB (forward, 5′-CCTGTTGG AGTCTGATCT-3′; reverse, 5′-TCCATTCACAGTGAGGAC-3′) and MEIS1 (forward, 5′-TACTTGTACCCCCCGCGAG-3′; reverse, 5′-TTTCTGCGCGAATCTGTTTG-3′). 18sRNA (forward, 5′-CCTGGATACCGCAGCTAGGA-3′; reverse, 5′-GCGGCGCAAT ACGAATGCCC-3′) was used as an endogenous control. These primers yielded 80-, 105-, 104-, 349-, 118- and 112-bp products, respectively.

Table 3
MiR-21 with clinicopathological factors of cervical carcinoma.

		negative	positive	X^2	P
Age (years)					
≤40	31	9	22	1.687	0.194
>40	53	9	44		
Tumor diameter					
≤4 cm	64	12	52	0.575	0.448[a]
>4 cm	20	6	14		
FIGO stage					
Ib	57	10	47	1.589	0.207
IIa	27	8	19		
Lymph nodal metastasis					
−	56	17	39	9.076	0.003
+	28	1	27		
Vessel invasion					
−	45	12	33	1.579	0.209
+	39	6	33		
Parametrial invasion					
−	73	17	56	0.456	0.499[a]
+	11	1	10		
Differentiation					
Mediate or well	37	15	22	14.346	<0.001
Poor	47	3	44		

[a] The probability is the results of continuity correction in chi-square test.

Table 4
The logistic regression analysis of miR-21 expression and SCC characteristics.

Variable	X^2	P	OR	95% CI of OR
Age grouping[a]	1.276	0.259	1.399	(0.781, 2.506)
Lymph nodal metastasis	3.93	0.047	0.137	(0.034, 0.545)
Differentiation	11.107	0.001	0.101	(0.026, 0.388)

[a] Age is control in this model.

2.5. Northern blotting

Oligonucleotide complementary to the mature miR-21 was 5′end labeled with [c-32P] adenosine triphosphate (ATP) by T4 kinase (TaKaRa). The blot was reprobed with a U6 snRNA probe as a loading control. Membranes were prehybridized and then hybridized at 37 °C for 24 h to a c-32P-labeled probe for miR-21 (5′-TCAACATCAGTCTGATAAGCTA-3′) or for U6 snRNA (5′-AAC GCTTCACGAATTTGCGT-3′). And Hela was used as a positive control.

2.6. Cell culture

The human cervical squamous cancer cell lines Caski and Siha, and the cervical adenocarcinoma cell line Hela were purchased from American Type Culture Collection and maintained in RPMI 1640 medium (Life Technologies) supplemented with 10% fetal bovine serum (Invitrogen). The Caski line is reported to contain an integrated human papillomavirus type 16 genome (HPV-16, about 600 copies per cell) as well as sequences related to HPV-18. The Siha line is reported to contain an integrated human papillomavirus type 16 genome (HPV-16, 1 to 2 copies per cell).

2.7. Cell transfection

Anti-miR-21 (Ambion) was transiently transfected into Caski and Siha cells with the siPORT NeoFx transfection reagent (Ambion). For mock transfection conditions, anti-miR miRNA was substituted with random oligonucleotides at equal concentrations. All experiments were completed in triplicate. At 48 h post-transfection, adherent cells were harvested and the levels of endogenous miR-21 were assessed by qRT-PCR as described above.

2.8. MTT assay

Cell survival was assessed using the 3-(4, 5-dimethylthiazol-2-yl)-2, 5-diphenyl-2H-tetrazolium bromide (MTT) assay (Sigma). MTT was added at a final concentration of 0.5 mg/mL at 48 h after transfection and cells were incubated for 4 h at 37 °C and dissolved in 150 μL of DMSO (Sigma). Optical density values were read at 570 nm (A570) using an Easy Reader 340 AT (SLT-Lab Instruments). Each experiment was carried out in triplicate and repeated three times.

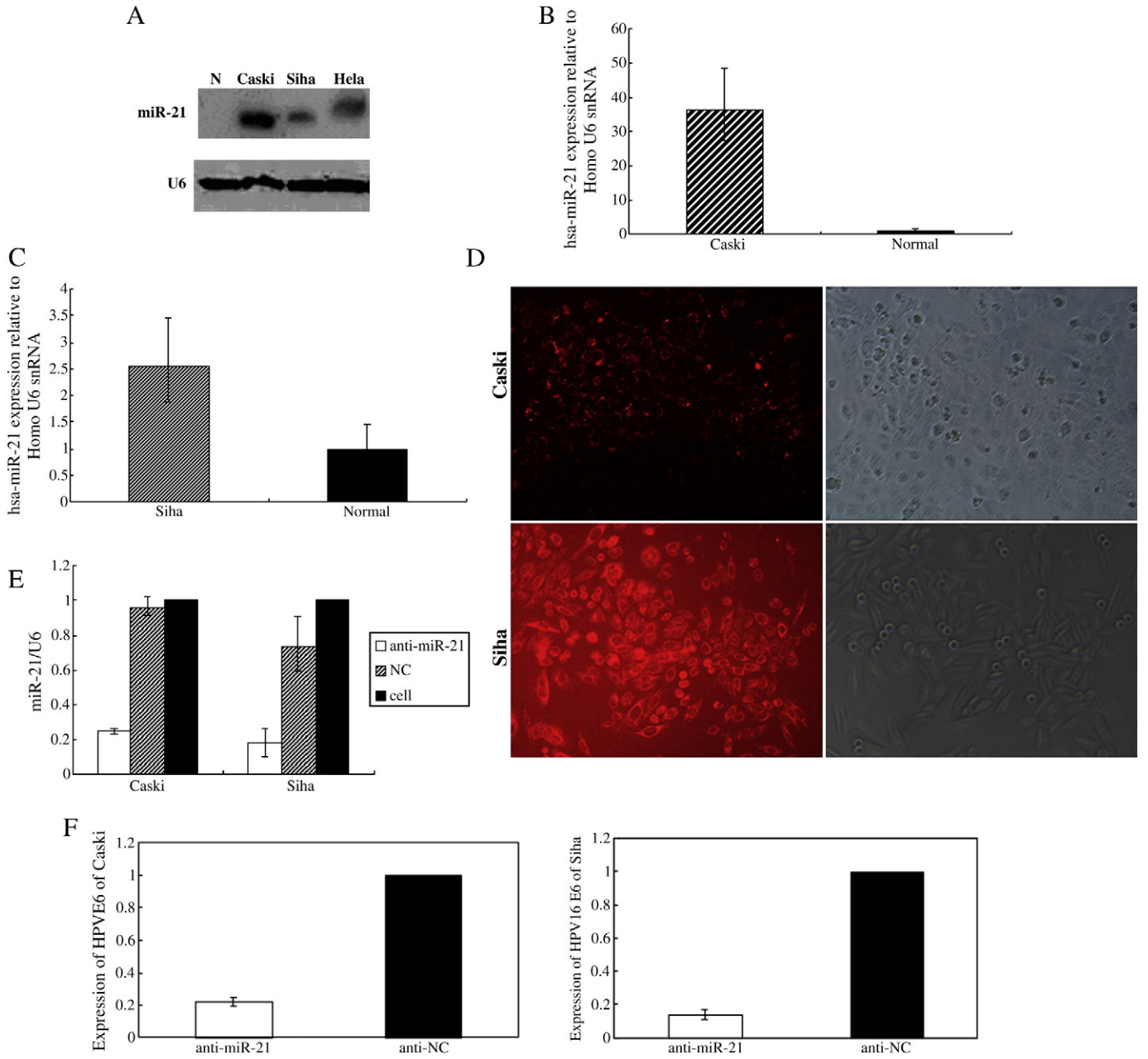

Fig. 2. Upregulation of miR-21 in SCC cell lines infected with HPV16. (A) Overexpression of miR-21 in SCC cell lines was compared with normal cervical tissues without HPV infection by Northern blotting. Lane 1 normal cervical tissues; lane 2 Caski; lane 3 Siha; lane 4 HeLa. (B) Comparison of the average expression level of miR-21 in Caski cell line and normal cervical tissues verified by qRT-PCR. (C) MiR-21 is highly expressed in the Siha cell line relative to normal cervical tissues, as verified qRT-PCR. (D) Microscopy images of cells following transfection (×400 magnification). (Up left) Control group of Caski cells under fluorescence microscopy; (up right) control group of Caski cells under light microscopy;(low left) control group of Siha cells under fluorescence microscopy; (low right) control group of Siha cells under light microscopy. (E) MiR-21 expression was quantified by qRT-PCR in transfected Caski and Siha cells. Expression of miR-21 was normalized to that of U6 snRNA. "NC" means Caski or Siha transfected with anti-miR negative control, while "cells" means Caski or Siha without any treatment. (F) Expression level of E6 in Siha cells was downregulated after inhibition of miR-21.

2.9. Annexin V analysis

Cell pellets were resuspended in Annexin V-FLUOS staining solution (Roche Molecular Biochemicals) and incubated for 15 min at room temperature. Samples were then analyzed on a FSCAN flow cytometer (Hershey Medical Center Core Facility).

2.10. Scratch migration assay

Confluent cells were transfected with anti-miR-21 or control oligonucleotides. At 48 h after transfection, a cell scratch spatula was used to make a scratch in the cell monolayer. Pictures of the scratches were taken (10× magnification) by using a digital camera system coupled with a microscope. The pictures were taken at 24 h.

2.11. Transwell cell migration assay

Forty-eight hours after transfection with anti-miR-21 inhibitors or control oligonucleotides, transfected cells were resuspended in serum-free RPMI 1640 medium and 5×10^4 cells were added to the upper chamber of Matrigel-coated 24-well plates (8 μm pore size, Corning, Corning, NY). The lower compartment was filled with RPMI 1640 medium containing 20% FBS. After 24 h, cells that had not migrated were removed from the upper face of the filters using cotton swabs, and cells that had migrated to the lower surface of the filters

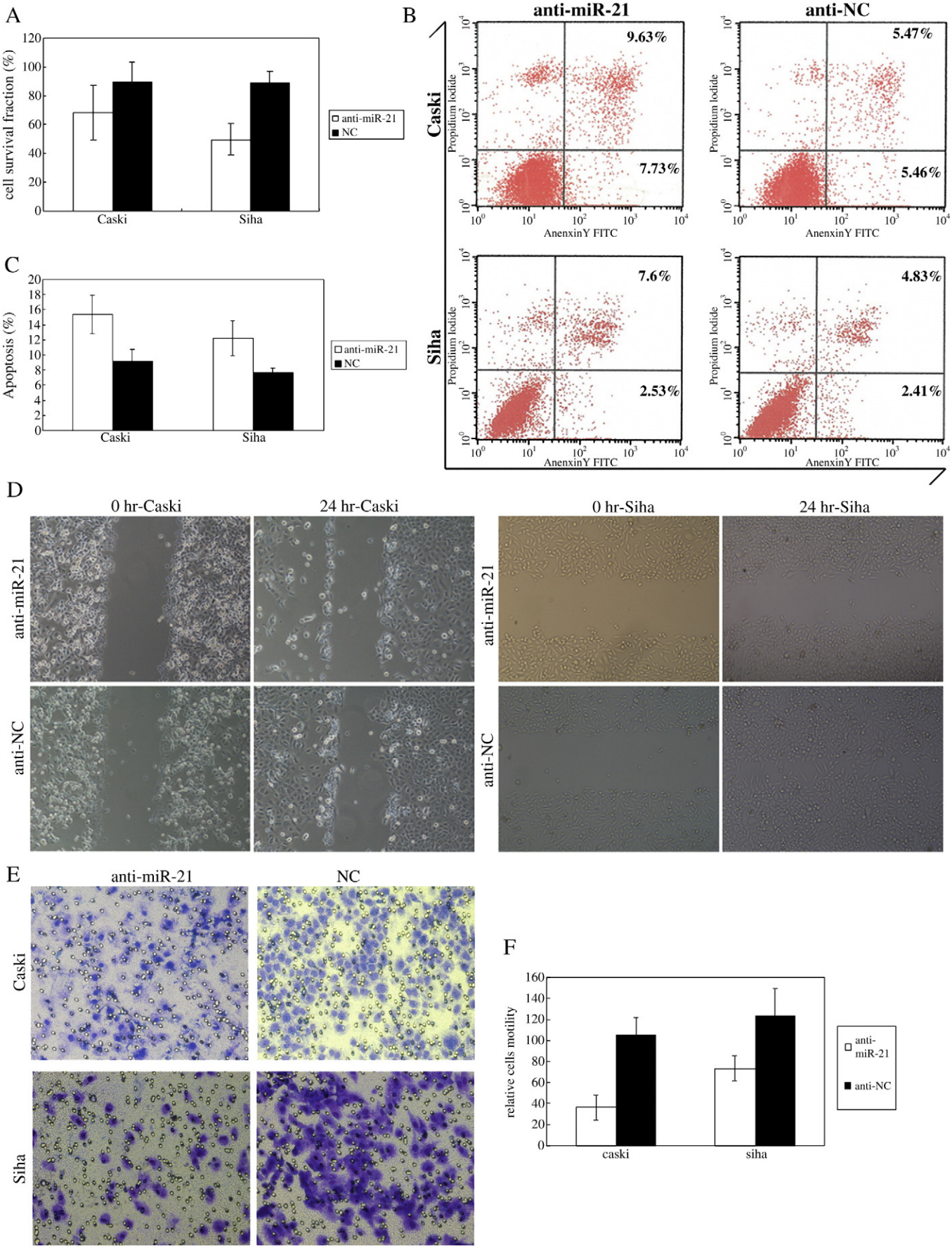
A
cell survival fraction (%)
anti-miR-21
NC
Caski
Siha
B
anti-miR-21
anti-NC
Caski
Siha
Propidium Iodide
AnenxinY FITC
9.63%
7.73%
5.47%
5.46%
7.6%
2.53%
4.83%
2.41%
C
Apoptosis (%)
anti-miR-21
NC
Caski
Siha
D
0 hr-Caski
24 hr-Caski
0 hr-Siha
24 hr-Siha
anti-miR-21
anti-NC
E
anti-miR-21
NC
Caski
Siha
F
relative cells motility
anti-miR-21
anti-NC
caski
siha

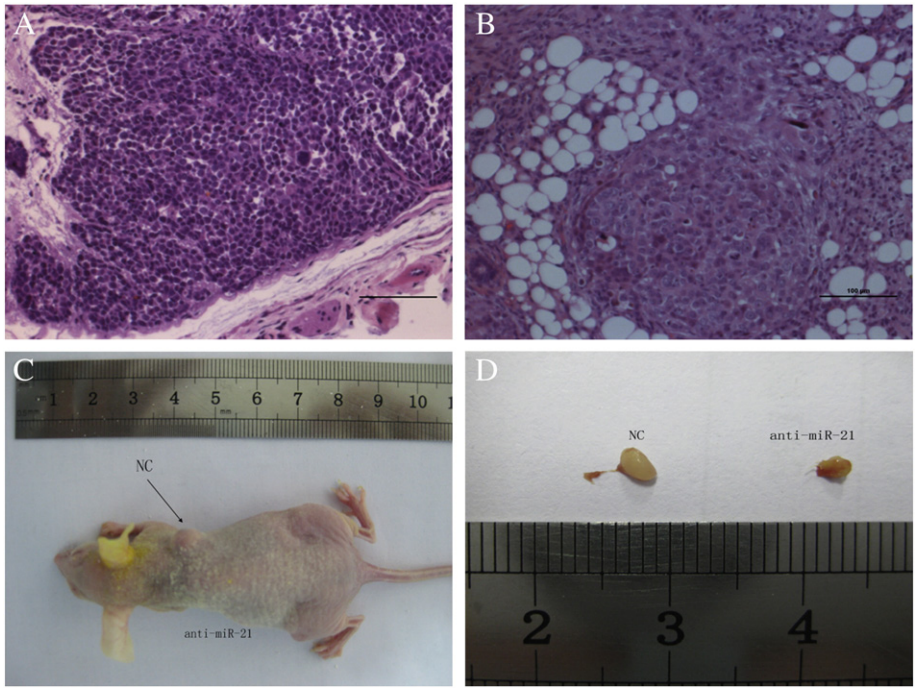

Fig. 4. Effect of miR-21 on tumor formation in a nude mouse xenograft model. (A) Tumor xenografts with anti-miR-21 (left) and NC. (B) (Right) have similar histologic structure evaluated by H&E staining (×200). (C) and (D) Anti-miR-21 reduced tumor formation.

were fixed in methanol and stained with crystal violet solution. Images of five different fields of view were captured from each membrane and the number of migrated cells was counted. The mean of triplicate assays for each experimental condition was calculated.

2.12. Tumor xenografts

Four-week-old female nude mice were cared for in accordance with the Guide for the Care and Use of Laboratory Animals (NIH publication nos. 80-23, revised 1996) and experiments were performed according to the institutional ethical guidelines for animal experiments. Siha cells (2×10^6) were transfected with anti-miR-21 or anti-miRNA Negative Control for 48 h. Cells were suspended in 200 μL PBS and then s.c. injected into either side of the posterior flank of the same female BALB/c athymic nude mouse. Six nude mice were used in our experiment. Tumor growth was examined every third day for 4 weeks. Tumor volume (V) was calculated by measuring the length (L) and width (W) with calipers and calculated with the formula $(L\times W^2)\times0.5$. Tumor xenografts were harvested and snap-frozen. Cryosections (4 μm) were stained with H&E.

Table 5
List of significantly changed mRNAs.

Positive genes	Fold change	Negative genes	Fold change
CCL20	13.60 ± 6.71	SLC7A7	−2.56 ± 2.07
ARC	12.89 ± 6.32	C15orf27	−2.44 ± 1.21
ss	6.85 ± 3.67	CPYAB	−2.38 ± 2.13
IL13RA2	6.79 ± 2.19	MATN2	−2.17 ± 1.07
IL24	6.34 ± 2.72	ALDH3A1	−1.92 ± 1.03
CRABP2	4.85 ± 0.79	NP_078839	−1.75 ± 0.29
IL6	4.65 ± 1.18	COL5A1	−1.75 ± 1.14
ACRC	4.22 ± 2.59	RBL1	−1.72 ± 0.76
FGF21	4.08 ± 1.55	WISP2	−1.72 ± 0.44
EGR1	3.43 ± 1.46	MEIS1	−1.69 ± 0.58

2.13. Microarray experiment

Total RNA of cells transfected with anti-miR-21 or scrambled RNA oligonucleotide was extracted using the TRIZOL Reagent (Invitrogen) according to the manufacturer's instructions. Gene-expression profiling was performed for each pooled RNA sample separately on the GeneChip_Porcine Genome Array (Affymetrix) [15] at CapitalBio Corporation (Beijing, China), in which the GeneChip microarray service was certificated by Affymetrix. Details of the probe set can be obtained at http://www.affymetrix.com/ products/arrays/index.affx. The protocol for microarray processing was carried out according to the GeneChip_Expression Analysis Technical Manual (Affymetrix, Rev.5, Part number 701021). A 1.5-fold or greater change in intensity was used as the criterion for inclusion in our filtered data set. The microarray data has been posted on the GEO database at NCBI. The accession number is GSM723046.

2.14. Bioinformatics

Potential miRNA targets were predicted and analyzed using five publicly available algorithms, miRanda (http://www.microrna.org), TargetScan (http://www.targetscan.org/), miRbase (http://www.mirbase.org/) and MAMI (http://mami.med.harvard.edu/). To reduce the number of false positives, only putative target genes predicted by at least three programs were accepted.

Fig. 3 MiR-21 affects proliferation, apoptosis and migration in vitro. (A) MiR-21 ASO specifically inhibits cell growth in SCC cell lines as determined by MTT assay. (B) Inhibition of miR-21 promotes apoptosis. Cell death is monitored by Annexin V staining and flow cytometry. The right lower quadrant of each plot contains early apoptotic cells, whereas the right upper quadrant contains late apoptotic cells. This experiment was repeated on three independent occasions, and similar results were obtained each time. (C) Each bar represents mean values ± SE from three independent experiments (right). (D) Effect of miR-21 on cell migration by scratch wound migration assay. At 24 h after scratching, cell migration was repressed in Caski (left) and Siha (right) cells by transfection with miR-21 inhibitor compared with the control. (E) Twenty-four hours after inhibition of miR-21, transwell analysis was applied in Caski cells (left) and Siha cells (right). Migrated cells were counted from five randomly chosen fields. (F) Ectopic expression of miR-21 influences tumor cell migration. Values are the average of triple determinations, with the S.D. indicated by error bars.

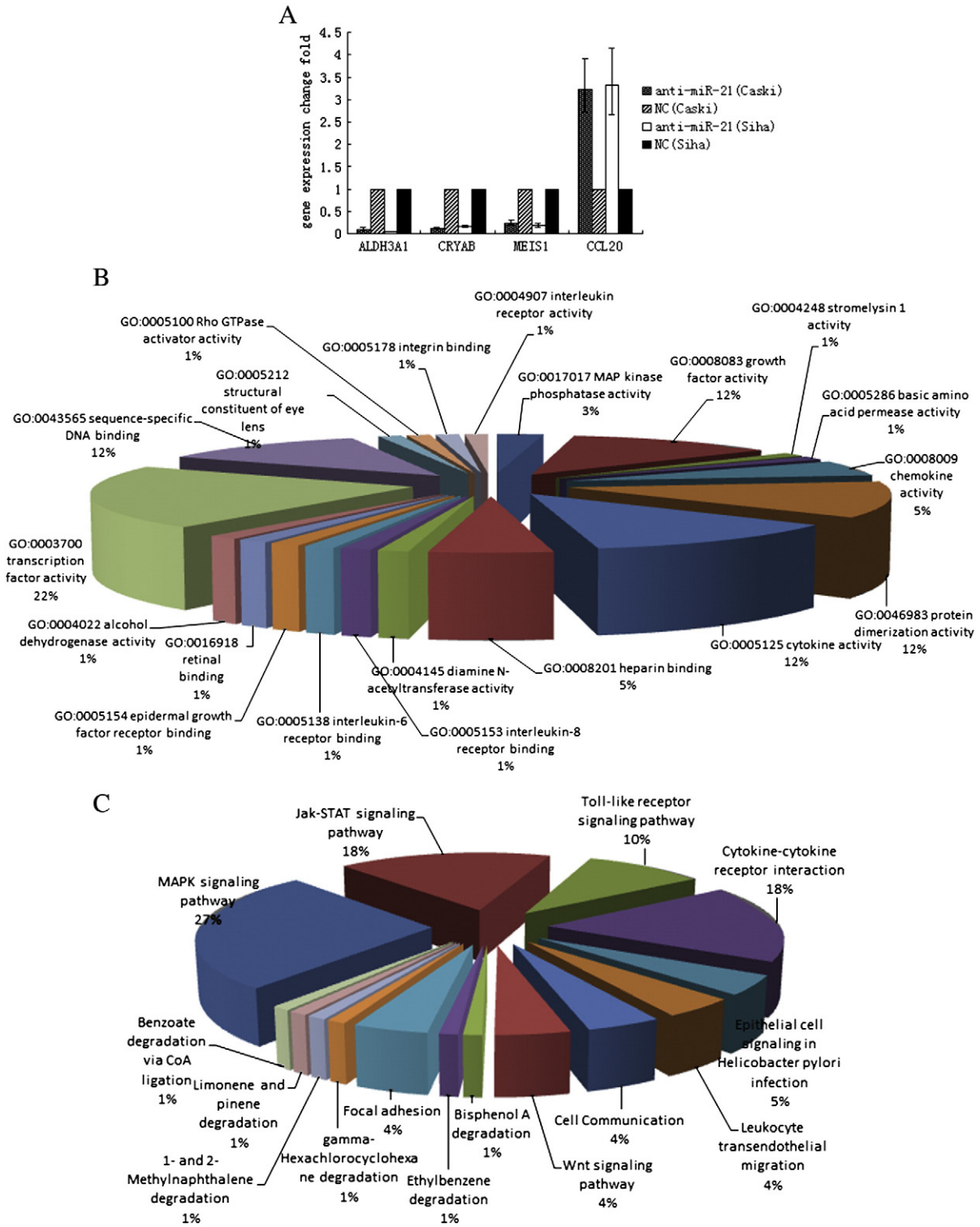

Fig. 5. (A) Microarray result was confirmed by qRT-PCR. (B)The molecular function of genes. (C) The analysis of KEGG.

2.15. Luciferase reporter assays

A fragment of 3′-UTR of CCL20 (primer F: 5′-CCGctcgagAAACTGTGGCTTTT CTGGAATGG-3′, primer R: 5′-ATAAGAATgcggccgcAACAGAAGAACTTTTTGT TTCTTTATTTTC-3′) containing putative binding sites for miR-21 was subcloned into psiCHECK-2 Vector (Promega, Madison, WI, USA) located 3′ to the Renilla luciferase translational stop codon. Mutant 3′-UTR, which carried a mutated sequence (primer F: 5′-CCGGAATTCcgctcgagAAACTGTGGCTTTTCTGGAATGG-3′, primer R: 5′-CGCGGATCCATAAGAAT gcggccgcAACAGAAGAACTTTTTGTTT CTTTATTTTC-3′) in the complementary site for the seed region of miR-21, was generated using the fusion PCR method. The nucleotide sequences of the constructed plasmids were confirmed by DNA sequencing analysis.

For luciferase reporter assays, HEK-293T cells (6×10^4) were seeded in 24-well plates and then cotransfected with 0.5 μg of psiCHECK-2-3′-UTR-WT or psiCHECK-2-3′-UTR-MUT, and miR-21 or negative control, using Lipofectamine 2000 (Invitrogen). Assays were performed 48 h

Table 6
The pathways changed genes involved ($P<0.05$).

Pathway	Changed genes
MAPK signaling pathway	DUSP5, JUN, FGF21, MYC, GADD45A
Jak-STAT signaling pathway	IL24, IL6, MYC, IL13RA2
Toll-like receptor signaling pathway	JUN, IL6, IL8
Cytokine–cytokine receptor interaction	IL24, IL6, CCL20, IL8
Epithelial cell signaling in *Helicobacter pylori* infection	JUN, IL8
Leukocyte transendothelial migration	CLDN4, IL8
Cell communication	KRTHA4, TNC
Wnt signaling pathway	JUN, MYC
Bisphenol A degradation	DHRS2
Ethylbenzene degradation	DHRS2
Focal adhesion	JUN, TNC
Gamma-hexachlorocyclohexane degradation	DHRS2
1- and 2-Methylnaphthalene degradation	DHRS2
Limonene and pinene degradation	DHRS2
Benzoate degradation via CoA ligation	DHRS2

after transfection using the Dual-Luciferase Reporter Assay System (Promega). Luciferase activity was detected by GloMax-Multi Detection System (Promega). The Renilla luciferase signals were normalized to the internal firefly luciferase transfection control. Transfections were done triplicately in independent experiments.

2.16. Immunofluorescence

Siha cells transfected with either anti-miR-21 or control oligonucleotides for 48 h were fixed using 4% paraformaldehyde (in PBS) for 15 min at room temperature. Cells were blocked in PBS containing 5% rabbit serum for 2 h at room temperature before incubation with primary antibody, goat anti-CCL20 (R&D, USA) overnight at 4 °C followed by secondary rabbit anti-goat IgG-FITC (1:200, Santa Cruz, USA) for 2 h at room temperature.

2.17. ELISA

The concentration of CCL20 in cell culture supernatants was quantified using an enzyme-linked immunosorbent assay (ELISA) detection kit (Quantikine, R&D Systems, Minneapolis, MN, USA), according to the manufacturer's instructions.

2.18. Statistics

All statistical analyses were carried out using SPSS for Windows version 13.0. All results are expressed as the mean ± SEM from at least three separate experiments. Difference testing between groups was performed using chi-square test as appropriate. Binary logistic regression was used for multivariate analysis to fit a model for those found significant by univariate analysis. All tests performed are two-sided. Differences were considered statistically significant at $P<0.05$.

3. Results

3.1. MiR-21 is overexpressed in SCC tissues

We quantified the expression of miR-21 in tumor samples from 24 SCC patients (No.61–No.84) and 19 CIN patients (No.85–No.103) by qRT-PCR (Fig. 1A). Relative to the adjacent noncancerous tissues, 23 of 24 (95.8%) SCC tissues revealed >50% upregulation in miR-21 level. MiRNA expression was relatively stable in the adjacent normal cervical tissues, while miR-21 was 3.57-fold higher in SCC as compared with corresponding non-tumor tissues. In turn, miR-21 in CIN was 1.4-fold higher. MiR-21 expression in SCC was much higher than that in CIN. These results suggest that miR-21 up-regulation may play a role in the progression of SCC.

3.2. Correlation between miR-21 expression and clinicopathological characteristics of CIN and SCC

By in situ hybridization, we found miR-21 expression demonstrated in 66/84 (No.1–No.84) (78.57%) of the SCC and far less in CIN cases (No.85–No.126) (11/42, 26.19%; Table 2). While most of the cancers demonstrated 1+ miR-21 expression, 24 had 2+ expression (Table 3) (Fig. 1B). In all cancer specimens, miR-21 expression was seen predominately in the cytoplasm of tumor cells and not in the surrounding stroma. Multivariate logistic regression analysis showed that miR-21 expression

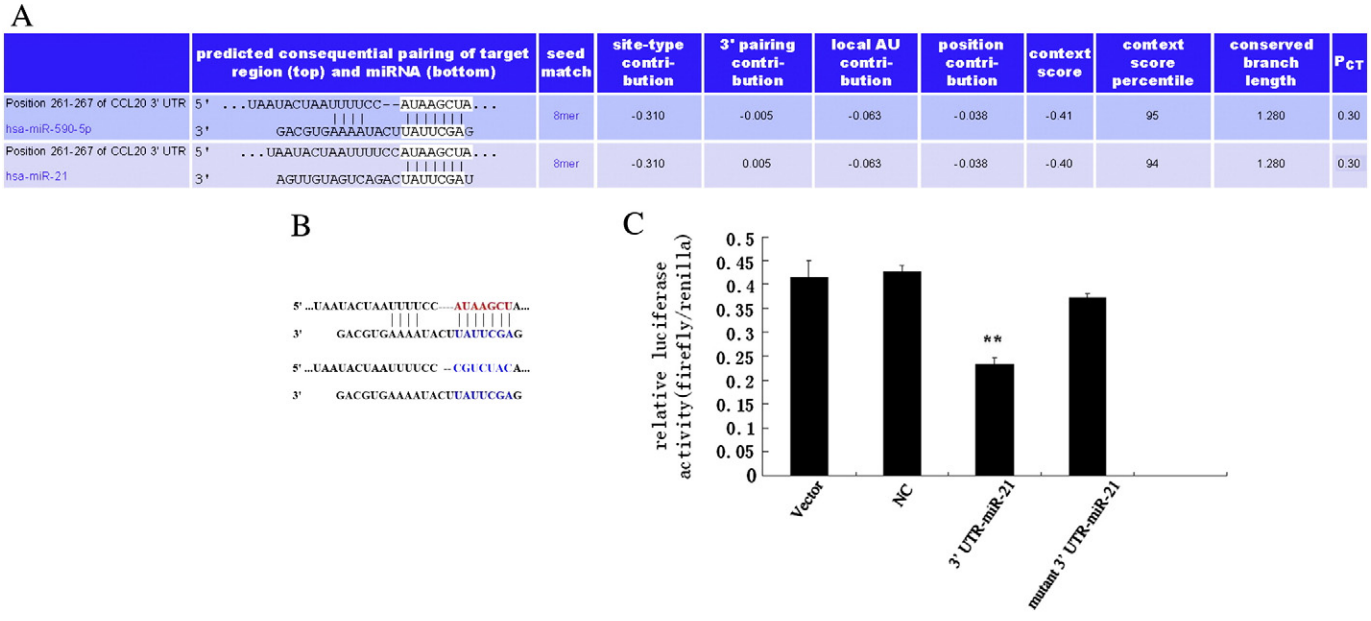

Fig. 6. CCL20 is a direct target of miR-21. (A) Putative miR-21-binding sequence in the 3′UTR of CCL20 mRNA. (B) A human CCL20 3′UTR fragment containing wild-type or mutated was cloned downstream of the luciferase reporter gene. (C) Luciferase analysis in HEK-293T cells. Luciferase activity on the presence of both wild-type CCL20 3′UTR or mutant and miR-21 (i.e., 3′UTR + miR-21) was compared with those of the controls (i.e., 3′UTR + vacant vector and 3′UTR + NC). $^{**}P<0.05$.

correlated with tumor differentiation and nodal status (Table 4). HPV16 infection was further confirmed by immunohistochemistry (Fig. 1C).

3.3. HPV16 infection may have a relationship with upregulation of miR-21 in SCC cell lines

To further investigate the machinery by which miR-21 contributes to SCC development, we used cultures of two cell lines, Caski and Siha and verified miR-21 overexpression by Northern blot using a miR-21-specific probe relative to the normal cervical tissues without HPV infection (Fig. 2A). In agreement with Northern blots, qRT-PCR showed that miR-21 expression was 36.42 fold higher in Caski cells (Fig. 2B) and 2.56-fold higher in Siha cells than that in normal cervical tissues uninfected with HPV (Fig. 2C).

The significant overexpression of miR-21 in SCC samples and cell lines prompted us to explore the possible biological significance of miR-21 in tumorigenesis. As an initial step, we transfected Caski and Siha cells with a 2′-O-methylated antisense miR-21 (anti-miR-21). And q-RT-PCR showed that transfection with anti-miR-21, but not anti-miRNA negative control, specifically knocked down miR-21 expression ($P<0.05$; Fig. 2D and E). We found the expression of HPV16E6 was downregulated after transfection with anti-miR-21 ($P<0.05$, Fig. 2F). This suggested that overexpression of miR-21 might be at least partly caused by HPV16 infection.

3.4. Inhibition of miR-21 reduces SCC cell proliferation in vitro

Cell proliferation is important for malignant progression, so we evaluated whether miR-21 contributes to SCC cell survival. After 48 h transfection, an MTT assay demonstrated that cell proliferation was significantly reduced upon transfection with anti-miR-21 (both $P<0.05$), but not with the unrelated negative control (Fig. 3A). These findings indicate that miR-21 is involved in the proliferation of SCC.

3.5. Knock-down of miR-21 promotes SCC cell apoptosis

To explore the mechanism underlying the tumor growth by miR-21, we then investigated the effect of miR-21 on Annexin V staining. Interestingly, apoptosis was substantially increased following knock-down of miR-21 (Fig. 3B and C).

3.6. Blocking of miR-21 negatively regulates cell migration

Next, the scratch wound migration assay was carried out to assess the effect of miR-21 on cell migration. We found that blocking of miR-21 activity led to a significant decrease in the motility of Caski cells and Siha cells (Fig. 3D and E). In order to validate the results, we analyzed cell migration by transwell method. The results were similar to the scratch wound migration assay ($P<0.05$. Fig. 3F).

3.7. MiR-21 ASO inhibits tumorigenesis of SCC xenografts

To further examine the effect of miR-21 on the in vivo growth of cervical carcinoma, anti-miR-21 and NC-transfected Siha cells were independently injected subcutaneously into either anterior flank of the same nude mouse. Compared to Siha cells transfected with NC miRNAs, the tissue structure and cell morphology of Siha cells transfected with anti-miR-21 did not differ (Fig. 4A and B), while the frequency of tumor formation was reduced (4/6 versus 1/6 Fig. 4C and D).

3.8. Microarray analysis shows transcripts are regulated by miR-21

We analyzed SCC cells transfected with anti-miR-21 and negative control respectively using 22 k human Genome Array (CapitalBio Corporation, Beijing, China). We observed that there were 99 transcripts upregulated at least 1.5 fold in Caski and Siha cells transfected with anti-miR-21 compared with negative control, while 71 transcripts were downregulated. The bulk of upregulated transcripts changed at the mRNA level, suggesting that miRNAs generally have a fine-tuning role in regulating gene expression.

In an effort to validate our array expression findings, four of the differentially expressed mRNAs (ALDH3A1, CRYAB, MEIS1 and CCL20) were chosen for qRT-PCR analysis. The trends for either up- or downregulation of mRNA expression were consistent by qRT-PCR measurement (Table 5) (Fig. 5A).

To explore the biological significance of the differentially expressed mRNA genes, we used pathway analysis software including KEGG (http://www.genome.ad.jp/kegg/), BioCarta (http://www.biocarta.com) and Genmapp (http://www.genmapp.org/). Additionally, Gene Ontology (http://www.geneontology.org/) was used to analyze the molecular function, biological process and cellular component of these mRNA genes. Pathway analysis identified a gene network associated with many biological processes. The biological processes most highly associated with this network were cell death, cellular growth, proliferation, and carcinogenesis (Table 6) (Fig. 5B–C).

3.9. MiR-21 targets CCL20

In an effort to further explore the biological relationship between the differentially expressed messenger- and miR-21 in our analysis, we performed a search for predicted messenger RNA targets of miR-21. We found that CCL20 was predicted to be a target of miR-21 by miRanda, TargetScan, miRbase and MAMI programs. Combining the target prediction bioinformatics with expression profiling, we identified CCL20, which was remarkably upregulated in miR-21 ASO treated cells, as a candidate target gene of miR-21.

Through sequence analysis, we further found that CCL20 mRNA contains a putative miR-21 binding site (Fig. 6A). To validate whether CCL20 is a bona fide target of miR-21, a human CCL20 3′UTR fragment containing wild-type was cloned downstream of the firefly luciferase reporter gene (Fig. 6B). Interestingly, the relative luciferase activity of the reporter that contained wild-type 3′UTR was significantly suppressed when pc3-miR-21 was cotransfected. However, the luciferase activity of the reporter containing the mutant miR-21-binding site

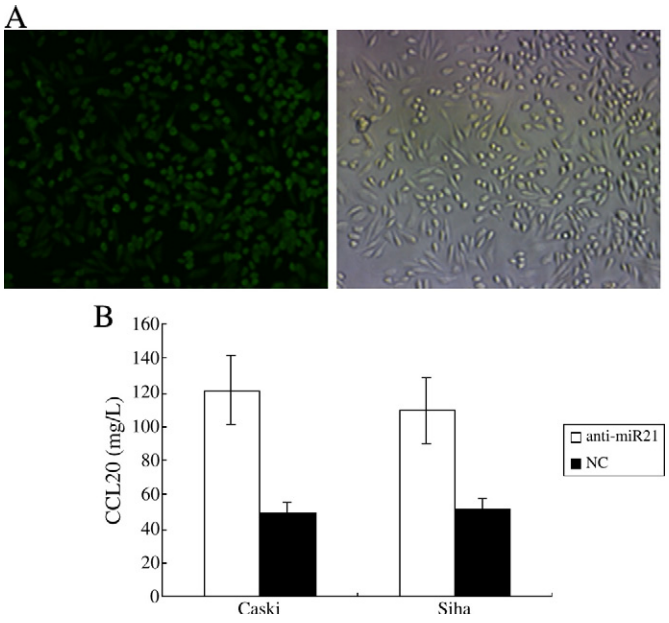

Fig. 7. Increased expression of endogenous CCL20 by miR-21. (A) Siha cells transfected with anti-miR-21 shows CCL20 in cytoplasm and intranuclear or perinuclear localization (green). (B) ELISA titering of CCL20 concentration in SCC cells with transfectants.

was unaffected, indicating that miR-21 may suppress gene expression through miR-21-binding sequences at the 3′-UTR of CCL20 gene (Fig. 6C). This suggests that miR-21 represses CCL20 expression by targeting the 3′UTR.

The effect of miR-21 on endogenous expression of CCL20 was further examined. qRT-PCR showed that inhibition of endogenous miR-21 by anti-miR21 resulted in upregulation of the CCL20 mRNA (Fig. 5A). Furthermore, the upregulation of protein expression was confirmed by immunofluorescence (Fig. 7A). Culture supernatants collected for use in ELISA analysis exhibited the same results (Fig. 7B).

4. Discussion

MiRNAs have been extensively studied in several cancers recently; however, understanding of the potential role of miRNAs in cervical cancer is still limited. Here, we showed that expression of miR-21 was significantly increased in cervical squamous cancer tissues and cell lines.

Consistent with previous findings from other cancers, we found that miR-21 could dramatically increase cell proliferation, inhibit apoptosis and promote cell migration in cervical squamous cancer lines. We also showed that overexpression of miR-21 was associated with advanced disease and lymph node metastasis. Therefore, our data indicate that miR-21 has multiple functions in the development of cervical squamous cancer.

By Merck Custom human expression array, we found that several chemokines involved in this study are potent signal transducers and regulators of gene expression implicated in carcinogenesis, especially for CCL20, which has been reported to be overexpressed in pancreatic carcinoma, oral squamous cell carcinoma and glioma [16–18]. However, CCL20 was found to be downregulated, together with other genes in the metastatic subpopulations of a human pulmonary adenocarcinoma cell line [19]. Recently, Lewis lung carcinoma (LLC) cells were shown to express low levels of CCL20 (LARC), both in vitro and in vivo. Furthermore, the local production of CCL20 proved to reduce the metastatic potential of the LLC line [20].

Quantitative and functional alterations of LCs have been reported in cervical SILs and correlated with a lower CCL20 expression in dysplastic epithelium. This result is in agreement with previous studies showing a deregulation of CCL20 secretion in cancers and non-tumor pathologies [21–27].

HPV infection is thought to be the most important factor for transition from normal cervical epithelium to pre-neoplastic cervical intraepithelial neoplasia that subsequently transforms to invasive cervical cancer. However, the pathogenic mechanism is still unknown. The miR-21 gene is located on chromosome 17q23.2, which is inside the common fragile site FRA17B. This region has been frequently found to be amplified in several solid tumors [28], which seems to be consistent with the fact that miR-21 is elevated in these cancers. Interestingly, one of the HPV16 integration loci is at 17q23.2 [29,30], thus it is intriguing to speculate that the expression of cellular miRNA genes at or near HPV integration sites may contribute to the tumor phenotype. Here, we have shown that expression of miR-21 was upregulated in patients with HPV infection, implying that HPV infection induces carcinogenesis probably through altering expression of some oncomiRs such as miR-21. HPV16 E6 and E7 oncoproteins are implicated in the down-regulation of CCL20 expression by HPV-transformed KC [31]. Our data suggested that CCL20 expression has a negative correlation with the expression of miR-21 in cervical tissues and cell lines at the transcriptional and protein level.

In conclusion, miR-21 is overexpressed in cervical squamous cancer, and aberrant expression of miR-21 can alter multiple biological processes in human cervical cancer cells such as proliferation, apoptosis, and migration, probably through regulating CCL20 and other critical target genes. MiR-21 can serve as a biomarker for cervical squamous cancer, and an inhibitory strategy against miR-21 or miR-21/CCL20 interaction will have a strong rationale for treatment for cervical squamous cancer. Moreover, eradication of HPV may be necessary for prevention of cervical squamous cancer.

Conflict of interest

The authors declare no conflict of interest.

Acknowledgements

This work was supported by National Natural Science Foundation of China (30672221, 30872743 and 81101979), Guangdong Province Natural Scientific Grant (6021279 and 2011040004639), Science Technology Planning Key Project of Guangdong Province (2009A030301006), Guangzhou Science and Technology Plan (2010J-E291) and Key Clinical Program of the Ministry of Health ([2010]439).

References

[1] R. Sankaranarayanan, J. Ferlay, Worldwide burden of gynaecological cancer: the size of the problem, Best Pract. Res. Clin. Obstet. Gynaecol. 20 (2006) 207–225.
[2] F. Bray, A.H. Loos, P. McCarron, E. Weiderpass, M. Arbyn, H. Møller, M. Hakama, D.M. Parkin, Trends in cervical squamous cell carcinoma incidence in 13 European countries: changing risk and the effects of screening, Cancer Epidemiol. Biomarkers Prev. 14 (2005) 677–686.
[3] C.Z. Chen, MicroRNAs as oncogenes and tumor suppressors, N. Engl. J. Med. 353 (2005) 1768–1771.
[4] L.F. Sempere, M. Christensen, A. Silahtaroglu, M. Bak, C.V. Heath, G. Schwartz, W. Wells, S. Kauppinen, C.N. Cole, 2007, Altered MicroRNA expression confined to specific epithelial cell subpopulations in breast cancer. Cancer Res. 67 (2007) 11612–11620.
[5] S. Volinia, G.A. Calin, C.G. Liu, S. Ambs, A. Cimmino, F. Petrocca, R. Visone, M. Iorio, C. Roldo, M. Ferracin, R.L. Prueitt, N. Yanaihara, G. Lanza, A. Scarpa, A. Vecchione, M. Negrini, C.C. Harris, C.M. Croce, A microRNA expression signature of human solid tumors defines cancer gene targets, Proc. Natl. Acad. Sci. U. S. A. 103 (2006) 2257–2261.
[6] M. Dillhoff, J. Liu, W. Frankel, C. Croce, M. Bloomston, MicroRNA-21 is overexpressed in pancreatic cancer and a potential predictor of survival, J. Gastrointest. Surg. 12 (2008) 2171–2176.
[7] A.J. Schetter, S.Y. Leung, J.J. Sohn, K.A. Zanetti, E.D. Bowman, N. Yanaihara, S.T. Yuen, T.L. Chan, D.L. Kwong, G.K. Au, C.G. Liu, G.A. Calin, C.M. Croce, C.C. Harris, MicroRNA expression profiles associated with prognosis and therapeutic outcome in colon adenocarcinoma, JAMA 299 (2008) 425–436.
[8] J. Li, H. Huang, L. Sun, M. Yang, C. Pan, W. Chen, D. Wu, Z. Lin, C. Zeng, Y. Yao, P. Zhang, E. Song, MiR-21 indicates poor prognosis in tongue squamous cell carcinomas as an apoptosis inhibitor, Clin. Cancer Res. 15 (2009) 3998–4008.
[9] Y. Chen, W. Liu, T. Chao, Y. Zhang, X. Yan, Y. Gong, B. Qiang, J. Yuan, M. Sun, X. Peng, MicroRNA-21 down-regulates the expression of tumor suppressor PDCD4 in human glioblastoma cell T98G, Cancer Lett. 272 (2008) 197–205.
[10] I.A. Asangani, S.A. Rasheed, D.A. Nikolova, J.H. Leupold, N.H. Colburn, S. Post, H. Allgayer, MicroRNA-21 (miR-21) post-transcriptionally downregulates tumor suppressor Pdcd4 and stimulates invasion, intravasation and metastasis in colorectal cancer, Oncogene 27 (2008) 2128–2136.
[11] Y. Hiyoshi, H. Kamohara, R. Karashima, N. Sato, Y. Imamura, Y. Nagai, N. Yoshida, E. Toyama, N. Hayashi, M. Watanabe, H. Baba, MicroRNA-21 regulates the proliferation and invasion in esophageal squamous cell carcinoma, Clin. Cancer Res. 15 (2009) 1915–1922.
[12] Q. Yao, H. Xu, Q.Q. Zhang, H. Zhou, L.H. Qu, MicroRNA-21 promotes cell proliferation and down-regulates the expression of programmed cell death 4 (PDCD4) in HeLa cervical carcinoma cells, Biochem. Biophys. Res. Commun. 388 (2009) 539–542.
[13] S.S. Liu, R.C. Leung, K.K. Chan, A.N. Cheung, H.Y. Ngan, Evaluation of a newly developed GenoArray human papillomavirus (HPV) genotyping assay and comparison with the Roche Linear Array HPV genotyping assay, J. Clin. Microbiol. 48 (2010) 758–764.
[14] A.M. Cheng, M.W. Byrom, J. Shelton, L.P. Ford, Antisense inhibition of human miRNAs and indications for an involvement of miRNA in cell growth and apoptosis, Nucleic Acids Res. 33 (2005) 1290–1297.
[15] S. Tsai, J.P. Cassady, B.A. Freking, D.J. Nonneman, G.A. Rohrer, J.A. Piedrahita, Annotation of the Affymetrix porcine genome microarray, Anim. Genet. 37 (2006) 423–424.
[16] J. Kleeff, T. Kusama, D.L. Rossi, T. Ishiwata, H. Maruyama, H. Friess, M.W. Büchler, A. Zlotnik, M. Korc, Detection and localization of Mip-3alpha/CCL20/Exodus, a macrophage proinflammatory chemokine, and its CCR6 receptor in human pancreatic cancer, Int. J. Cancer 81 (1999) 650–657.
[17] T. Kimura, H. Takeshima, N. Nomiyama, T. Nishi, T. Kino, M. Kochi, J.I. Kuratsu, Y. Ushio, Expression of lymphocyte-specific chemokines in human malignant glioma: essential role of LARC in cellular immunity of malignant glioma, Int. J. Oncol. 21 (2002) 707–715.
[18] Y. Abiko, M. Nishimura, K. Kusano, K. Nakashima, K. Okumura, T. Arakawa, T. Takuma, I. Mizoguchi, T. Kaku, Expression of MIP-3alpha/CCL20, a macrophage

inflammatory protein in oral squamous cell carcinoma, Arch. Oral Biol. 48 (2003) 171–175.
[19] A. Gemma, K. Takenaka, Y. Hosoya, K. Matuda, M. Seike, F. Kurimoto, Y. Ono, K. Uematsu, Y. Takeda, S. Hibino, A. Yoshimura, M. Shibuya, S. Kudoh, Altered expression of several genes in highly metastatic subpopulations of a human pulmonary adenocarcinoma cell line, Eur. J. Cancer 37 (2001) 1554–1561.
[20] A. Sutherland, J.F. Mirjolet, A. Maho, M. Parmentier, Expression of the chemokine receptor CCR6 in the Lewis lung carcinoma (LLC) cell line reduces its metastatic potential in vivo, Cancer Gene Ther. 14 (2007) 847–857.
[21] D. Bell, P. Chomarat, D. Broyles, G. Netto, G.M. Harb, S. Lebecque, J. Valladeau, J. Davoust, K.A. Palucka, J. Banchereau, In breast carcinoma tissue, immature dendritic cells reside within the tumor, whereas mature dendritic cells are located in peritumoral areas, J. Exp. Med. 190 (1999) 1417–1426.
[22] A. Bernat, N. Avvakumov, J.S. Mymryk, L. Banks, Interaction between the HPV E7 oncoprotein and the transcriptional coactivator p300, Oncogene 22 (2003) 7871–7881.
[23] A. Izadpanah, M.B. Dwinell, L. Eckmann, N.M. Varki, M.F. Kagnoff, Regulated MIP-3alpha/CCL20 production by human intestinal epithelium: mechanism for modulating mucosal immunity, Am. J. Physiol. Gastrointest. Liver Physiol. 280 (2001) G710–G719.
[24] T.F. Kimsey, A.S. Campbell, D. Albo, M. Wilson, T.N. Wang, Co-localization of macrophage in inflammatory protein-3alpha (Mip-3alpha) and its receptor, CCR6, promotes pancreatic cancer cell invasion, Cancer J. 10 (2004) 374–380.
[25] T. Nakayama, R. Fujisawa, H. Yamada, T. Horikawa, H. Kawasaki, K. Hieshima, D. Izawa, S. Fujiie, T. Tezuka, O. Yoshie, Inducible expression of a CC chemokine liver- and activation-regulated chemokine (LARC)/macrophage inflammatory protein (MIP)-3 alpha/CCL20 by epidermal keratinocytes and its role in atopic dermatitis, Int. Immunol. 13 (2001) 95–103.
[26] C. Rubie, V. Oliveira-Frick, B. Rau, M. Schilling, M. Wagner, Chemokine receptor CCR6 expression in colorectal liver metastasis, J. Clin. Oncol. 24 (2006) 5173–5174.
[27] M. Schmuth, S. Neyer, C. Rainer, A. Grassegger, P. Fritsch, N. Romani, C. Heufler, Expression of the C–C chemokine MIP-3 alpha/CCL20 in human epidermis with impaired permeability barrier function, Exp. Dermatol. 11 (2002) 135–142.
[28] G.A. Calin, C.M. Croce, Chromosomal rearrangements and microRNAs: a new cancer link with clinical implications, J. Clin. Invest. 117 (2007) 2059–2066.
[29] E.C. Thorland, S.L. Myers, B.S. Gostout, D.I. Smith, Common fragile sites are preferential targets for HPV16 integrations in cervical tumors, Oncogene 22 (2003) 1225–1237.
[30] E.C. Thorland, S.L. Myers, D.H. Persing, et al., Human papillomavirus type 16 integrations in cervical tumors frequently occur in common fragile sites, Cancer Res. 60 (2000) 5916–5921.
[31] J.C. Guess, D.J. McCance, Decreased migration of Langerhans precursor-like cells in response to human keratinocytes expressing human papillomavirus type 16 E6/E7 is related to reduced macrophage inflammatory protein-3alpha production, J. Virol. 79 (2005) 14852–14862.